



HAL
open science

Influence of the N atom and its position on electron photodetachment of deprotonated indole and azaindole

Jennifer A. Noble, Ernesto Marceca, Claude Dedonder, Christophe Juvet

► To cite this version:

Jennifer A. Noble, Ernesto Marceca, Claude Dedonder, Christophe Juvet. Influence of the N atom and its position on electron photodetachment of deprotonated indole and azaindole. *Physical Chemistry Chemical Physics*, 2020, 10.1039/D0CP03609A . hal-03031004

HAL Id: hal-03031004

<https://hal.science/hal-03031004>

Submitted on 30 Nov 2020

HAL is a multi-disciplinary open access archive for the deposit and dissemination of scientific research documents, whether they are published or not. The documents may come from teaching and research institutions in France or abroad, or from public or private research centers.

L'archive ouverte pluridisciplinaire **HAL**, est destinée au dépôt et à la diffusion de documents scientifiques de niveau recherche, publiés ou non, émanant des établissements d'enseignement et de recherche français ou étrangers, des laboratoires publics ou privés.

Influence of the N atom and its position on electron photodetachment of deprotonated indole and azaindole

Jennifer A. Noble^{1*} Ernesto Marceca², Claude Dedonder¹ and Christophe Jouvot¹

1 CNRS, Aix Marseille Univ., PIIM, Physique des Interactions Ioniques et Moléculaires, UMR 7345, 13397, Marseille, France. jennifer.noble@univ-amu.fr

2 INQUIMAE (CONICET – Universidad de Buenos Aires), DQIAQF (Facultad de Ciencias Exactas y Naturales, Universidad de Buenos Aires), Ciudad Universitaria, 3er piso, Pab. II, 1428 Buenos Aires, Argentina

Abstract

Electron photodetachment of cold deprotonated indole and azaindole anions has been studied by use of a mass-selective photofragmentation spectrometer capable of negative ion and neutral particle detection. The electron affinities of the indolyl radical and the 5-, 6- and 7-azaindolyl radicals have been measured with an uncertainty of less than 0.002 eV. The presence of the nitrogen atom in the six-membered ring of the azaindole anions stabilises the electron by 0.3 to 0.4 eV, i.e. about 10-15 %, compared to the indole anion. No fragmentation was observed in either the anionic or radical forms of the species studied. The appearance of dipole-bound states in the spectra of deprotonated 6- and 7-azaindole anions allowed us to analyse the vibrational structure of the neutral 6- and 7-azaindolyl radicals produced following photodetachment. Although no dipole-bound states were clearly identified for deprotonated indole or 5-azaindole, the shape of the photodetachment threshold suggests the presence of a very weakly dipole-bound state or dipole resonance, which cannot be resolved with our laser resolution.

Introduction

The bicyclic molecule indole (C_8H_7N) is the chromophore of tryptophan (Trp), one of the aromatic amino acids responsible for the fluorescence of proteins. Indolic systems are utilised in spectroscopic studies of biological interest and have been used to probe protein folding/unfolding dynamics, substrate binding, and external quencher accessibility¹. Green fluorescent proteins (GFP) have become established as efficient, non-invasive molecular instruments in cell biology and biomedicine. They are used for the visualisation and monitoring of internal processes within cells and whole organisms². All wild-type fluorescent proteins studied to date have a tyrosine (Tyr) as the central residue of the chromophore-forming triad. Usually, the phenolic hydroxyl of the chromophore Tyr ionises easily, giving rise to longer wavelength fluorescence (from green to far red) compared with FPs containing neutral Tyr. Replacement of Tyr by Trp results in a shift in fluorescence to shorter wavelengths in the cyan/green region. Tryptophan-based chromophores in fluorescent proteins can exist in an anionic charge state. Switching between protonated and deprotonated Trp in fluorescent proteins represents a new unexplored way to control their spectral properties.³ It is therefore interesting to study the optical properties of indole and indole derivatives in different charge states. Biocompatible azaindole isomers ($C_7H_6N_2$), characterised by different nitrogen-atom positions in the heterocycle, have recently emerged as promising indolic chromophores⁴ because the strong isomer dependent changes in their optical properties would allow tuning of the protein fluorescence.

Recently, the indolide anion (deprotonated indole) has been characterised and its adiabatic detachment energy (ADE = 2.4315 eV) measured via photoelectron spectroscopy⁵. However, to our knowledge, there is, to date, no measurement of the ADE of the azaindolide isomers (i.e. producing the dehydrogenated azaindole radicals). By comparison to previous studies of similar deprotonated species^{5,6}, particularly given that the excited states of indolide are low in energy compared to those in phenol⁷, one might expect to see competition between ionic fragmentation and photodetachment, as was observed for naphtholate⁸. The *n*-azaindole compounds (hereafter denoted as *n*-AI), in particular 7-AI, are also benchmarks for studying the excited proton/hydrogen transfer in 7-AI(H₂O)_{*n*}^{9,10,11} or 7-AI(NH₃)_{*n*}¹² clusters. Depending on whether this reaction is a proton or a hydrogen atom transfer through the molecular solvent (H₂O, NH₃) wire, the intermediate state will be, respectively, a deprotonated species or a dehydrogenated radical. However, neither of these species have yet been studied. Moreover, regarding the (7-AI)₂ dimer, the question of whether a concerted or a sequential excited state proton transfer takes place has given rise to long debate and generated strong controversy. In the case of a sequential process, the transient species correspond to protonated 7-AI on one side and deprotonated 7-AI on the other, again neither of which have been studied yet.

Here we present results on deprotonated 7-AI (hereafter denoted as [7-AI-H]⁻, where the removed proton is explicitly indicated) upon photon absorption, while the study of protonated 7-AI (7-AIH⁺) was addressed in another paper [ref Noble+2020 AIH+]. We have also studied the effect of the position of the N-atom on the electron affinity of the azaindoly radical ([*n*-AI-H]^{*}) for *n* = 5, 6 and 7, as well as comparing [*n*-AI-H]⁻ to deprotonated indole, [I-H]⁻. As will be seen, if the dipole moment of the dehydrogenated radical is large enough, our spectroscopic approach reveals the existence of a dipole-bound state (DBS). In such a state, the unpaired electron is only slightly bound to the neutral molecular core, and for this reason the structure of the dipole-bound core does not differ from that of the deprotonated radical.^{13,14} Consequently, the vibrational structure of the (aza)indoly radical in the ground state can be deduced from the spectroscopy of the dipole-bound anion.

An important question arises as to whether the radical will fragment after detachment. We recently studied the photodetachment of deprotonated aromatic amino acids¹⁵ and observed that the radical obtained after the ejection of the electron is unstable if the anion is deprotonated on the carboxyl group and stable if deprotonation occurs on the aromatic ring. We concluded that due to the flexibility of the amino-acidic moiety, no evidence of a clear photodetachment threshold nor of DBSs was seen in the spectra.

The questions we want to answer in this paper are:

Is there a competition between anion photofragmentation and electron photodetachment in *n*-azaindolide and indolide anions?

Is there fragmentation in the radical after photodetachment and, if so, is there a barrier to fragmentation?

What are the influences of the N-atom and its position in the six-membered ring of azaindole on the electron binding energy of the deprotonated chromophore?

Are there dipole-bound states, how stable are they, and are there dipole resonances evidenced in the spectra of *n*-azaindolide and indolide anions? DBSs are stable and well characterised when the dipole of the radical is larger than 4D.^{13,14,16,17,18,19,20} One can therefore ask oneself: what is the nature of these states when the dipole is just at the limit of stabilisation? By changing the N position, one can vary the dipole moment while keeping a very similar overall molecular structure.

Experimental methods and calculations

In contrast to most of the experiments in which the study of anions relies on photoelectron spectroscopy^{21–24, 5, 7, 25–27}, our experiment is centred upon the detection of the neutral counterpart(s). The advantage of the method is that the fragmentation of the radical issued from the photodetachment can be studied, while the drawback is that no information can be obtained on the kinetic energy of the detached electron. The experimental setup used for cold ion photofragmentation spectroscopy has been described in previous publications^{28, 29, 30} and has recently been modified to detect negative ions and neutral particles^{6, 15, 30}. Deprotonated indole and *n*-azaindole (*n* = 5, 6, 7) were produced in an electrospray ionisation (ESI) source by injecting a solution of the molecule at 10⁻⁴ M in a 5:1 methanol: water mixture.

The ions produced in the ESI are injected into the cryogenic ion trap just after a helium pulse has been introduced. The ions are stored in the cold trap for a few tens of ms, the time necessary to cool them to c.a. 50 K and for the subsequent reduction of the pressure in the trap. The ions are then extracted and accelerated at 3 kV. After passing the accelerating grid, the ions enter the “Gauss” tube set at the accelerating grid potential and, once they are inside, the tube potential is switched to ground. The ions then travel in the field free region of the time of flight mass spectrometer with a kinetic energy imposed by the accelerating voltage and are referenced to the ground potential. After 1 m of flight, they enter the post accelerating/decelerating “box”, after which the ions (or neutrals) are detected with a MCP detector³¹.

The laser used for photodissociation or photodetachment of the ions is a tunable OPO laser (EKSPLA) (10 Hz repetition rate, 10 ns pulse width, and a spectral resolution of ~10 cm⁻¹). The laser can interact with the ions in two different parts of the setup: either in the ion trap, which allows monitoring of the photodissociation process - leading to a fragment ion and a neutral fragment - by extracting the ions after the laser shot, or in the Gauss tube. In the latter case, since the precursor ions have been accelerated, the precursor neutral radicals produced by photodetachment and/or any neutral product fragments can be detected by the MCP. The laser interacts only once with the ion cloud, the signal is averaged over (usually) 8 shots at each wavelength and the spectra are recorded ten times and then averaged (occasionally, signal intensity and source stability allow us to perform shorter averaging). No smoothing procedure was used and thus the noise is due either to statistical uncertainty or the instability of the source.

The intact precursor radical will arrive at the same time as the anion precursor and the signal will be as narrow as the anion signal. In contrast, the neutral fragments will travel with the kinetic energy of the precursor ion plus the kinetic energy (positive or negative) released in the dissociative process and, for that reason, they will be observed at the same time-of-flight as the precursor, but exhibit peak broadening due to the kinetic energy released. To discriminate between the precursor anion and the neutral photodetached radical, two methods can be used:

- a) Decelerating the anions by applying high voltages (1.2 kV) in the accelerating/decelerating “box” (when a negative voltage is applied, the ions are decelerated in the box and will travel slower than the neutrals, thus arriving at the detector somewhat later than the neutrals).
- b) Maintaining the high voltage on the Gauss tube (instead of switching it to ground during the transit of the ions) in order to decelerate the anions at the output of the tube and prevent them reaching the detector, while the neutrals are not perturbed. This method minimises the time and the distance

travelled by the parent ions and thus minimises the background signal caused by neutral fragments produced by collisions between parent ions and the residual gas.

Using this method (already applied to the aromatic amino acids³² and to benzoic acid⁶) the anions were excited once they had been accelerated outside the trap, and the setup was configured to detect neutral particles. Since any neutral fragments formed following photodetachment will have some additional kinetic energy, they can easily be discriminated from the undissociated precursor radical produced by photodetachment (which appears as a narrow peak at the time corresponding to the mass of the precursor anion).

Compared to many other experiments^{33,34,35,36,37} the use of a cold trap^{38,39,40,41} has many advantages, as already shown by the Wang's group and others^{7,19}. Structured DBSs can be clearly seen and this gives information on the radical's structure with a high precision. If one has a narrow band laser, one can also get information on the auto ionization speed¹⁹. Moreover cooling allows one to follow the vibrational structure of the anion excited state when the fragmentation of autoionisation is not very fast^{19,207} (faster than 10 fs). The direct detection of fast neutrals can have the same sensitivity as the detection of ions^{31,37,42,43}. Moreover, this sensitivity allows ion/neutral or electron/neutral coincidence experiments^{44,45,22}; however, owing to the high repetition rate (KHz or more) necessary to perform coincidence experiments,^{44,45,22} there is not enough time to cool down the ions and thus the internal energy of the precursor cannot be known accurately. Measuring the formation of neutrals via the depletion of the precursor ion signal^{46,47,36} is not a very sensitive method, since one is dealing with a small signal on a large background and depends strongly on the stability of the source. In our case, the signal is essentially on a zero background and thus the sensitivity is orders of magnitude larger. Concerning DBSs, our resolution is similar to the resolution of SEVI²⁴ and is basically limited by the laser band width ($\sim 10\text{cm}^{-1}$).

We used the DFT method implemented in the Gaussian⁴⁸ package with the CAM-B3LYP/aug-cc-pVDZ functional to calculate the adiabatic detachment energies (ADE), the dipole moments of the dehydrogenated radicals, and the vibrations of both the deprotonated anions and dehydrogenated radicals in order to calculate the difference in zero-point energy (ΔZPE) between the two species. Although this method is far from perfect, other methods such as RI-MP2 or CC2 gave erratic results and have not been taken into account in the analysis. It should be noted that the calculated ΔZPE s are very small (0.01 eV or less) and since they lie well below the uncertainty of the calculation methods employed they will not be discussed further. The Franck-Condon simulations are performed using the pGopher software⁴⁹

Results

-Fragmentation of $[n\text{-Al-H}]^-$ and $[\text{I-H}]^-$ anions.

In order to investigate the possible photofragmentation of $[n\text{-Al-H}]^-$ and $[\text{I-H}]^-$ anions, they were photoexcited inside the cold ionic trap with the intention of monitoring parent anions and any anionic fragments. Nevertheless, no anionic fragments were detected using excitation wavelengths from the visible (700 nm) to the UV (225 nm). The sensitivity of our fragment detection is quite high and depends on the precursor ion signal, but it can reach 0.1%; to be conservative, the fragmentation in these cases is less than 1%.

In many experiments performed at room temperature,^{33,34,35,37,50} fragmentation is a minor channel, and this is due to an experimental artifact. Photo fragmentation (PF) efficiency is mostly controlled by the temperature of the ions (which may be higher than that of the trap). This is very easy to see for protonated species, where the spectra are well resolved at low temperature. For hot molecules, the ground state population is spread over many rovibrational levels and the laser excitation can only interact with a small part of the ion population, leading to an inefficient excitation and thus fragmentation. In our own experiment, the PF efficiency between the cooled and non-cooled trap varies significantly; we observe an increase of around two orders of magnitude when the laser sits on a band and when the trap is cold. For anions, PD is a continuum and thus is not influenced by the temperature (except very near the ADE) whereas the anions' excitation is temperature sensitive. Thus, the low fragmentation efficiency often measured is due to the drawbacks of hot traps rather than to molecular properties. In our case, the absence (with a detection limit below 1%) of fragments from cold ions is related to the fact that aromatics without substituents are hard to break and that the anions' excited states are quite high in energy. Since PD become faster as the energy increases, this favours PD over PF in a cold trap.

-Fragmentation of [n-AI-H] and [I-H]* radicals.*

The anions were photoexcited once they had been accelerated outside the trap, and the setup was configured to detect neutral particles. In this configuration, no neutral product fragments were detected, only the undissociated neutral radical, and thus we can conclude that the indolyl and azaindolyl radicals are quite stable, in agreement with our previous work in which dehydrogenation occurred on the indole ring of the amino acid tryptophan.¹⁵

-Photodetachment action spectra by detection of neutrals.

Photodetachment (PD) spectra were measured by following the yield of [I-H]* and [n-AI-H]* neutral radicals as the laser was scanned.

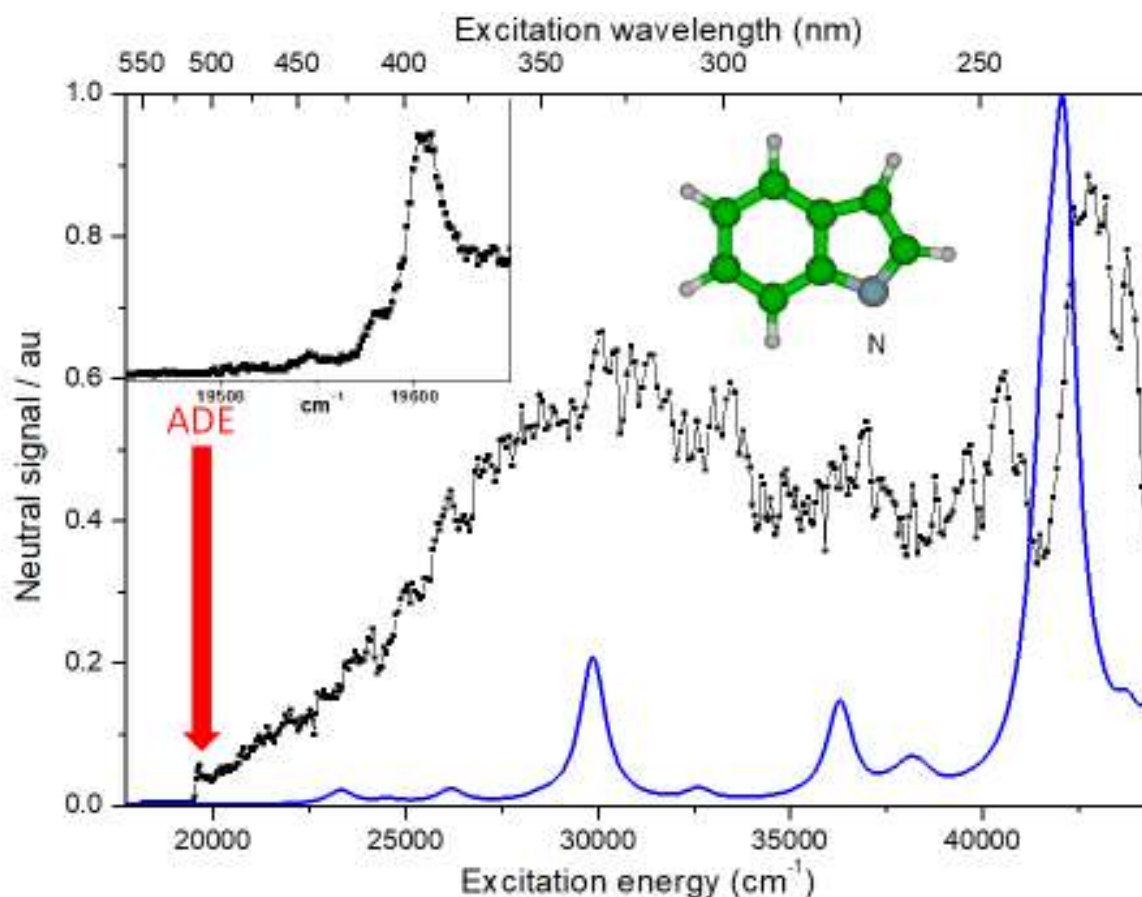


Figure 1: PD spectrum of the indolide anion recorded by following the yield of the indolyl $[I-H]^{\bullet}$ neutral over a wide spectral range (black). The arrow indicates the PD threshold, while the insert gives an expanded view of the threshold region. The calculated vertical electronic spectrum (at the CAM-B3LYP/aug-cc-pVDZ level) convolved by a Lorentzian function is shown in blue. There are some similarities with the experimental data. The intense band above 40 000 cm^{-1} is the 19th excited state; this shows that the electronic structure is quite congested.

The photodetachment spectrum of the indolide anion is presented in Figure 1. No DBSs could be observed, in contrast with the case of 6- and 7-azaindolides (vide infra). The strong band at 45000 cm^{-1} (235 nm) has been assigned to an excited state of the anion. This is the only excited state which can be clearly identified in the spectrum. Here, we note that the noise arising from the instability of the source and the laser could not be suppressed despite long-term averaging. Based on the calculations performed, there are probably other excited states which cannot be visually extracted from the continuum noisy photodetachment signal (see Figure S1 and the discussion below).

The photodetachment threshold measured for indolide in the experiment is $\text{ADE} = 2.430 \pm 0.001$ eV, which is in very good agreement with that measured by Nelson et al⁵ (2.4315 eV). At lower energy, a weak step can be observed and is assigned to the presence of hot bands, probably excited by collisional processes occurring during the extraction from the trap. The shape of the threshold is not one we would expect from the Wigner threshold law, in particular it should not exhibit such a peak-like profile just above the threshold. According to the Wigner threshold law⁵¹, *s*-wave detachment channels from π -type orbitals should have significant intensities near the detachment threshold leading to step function signals, as those we see for the 6- and 7-azaindolide anions (vide infra). In addition, since DBS bands are not present, no information on the vibrational spectroscopy of the indolyl radical can be obtained with our experimental setup.

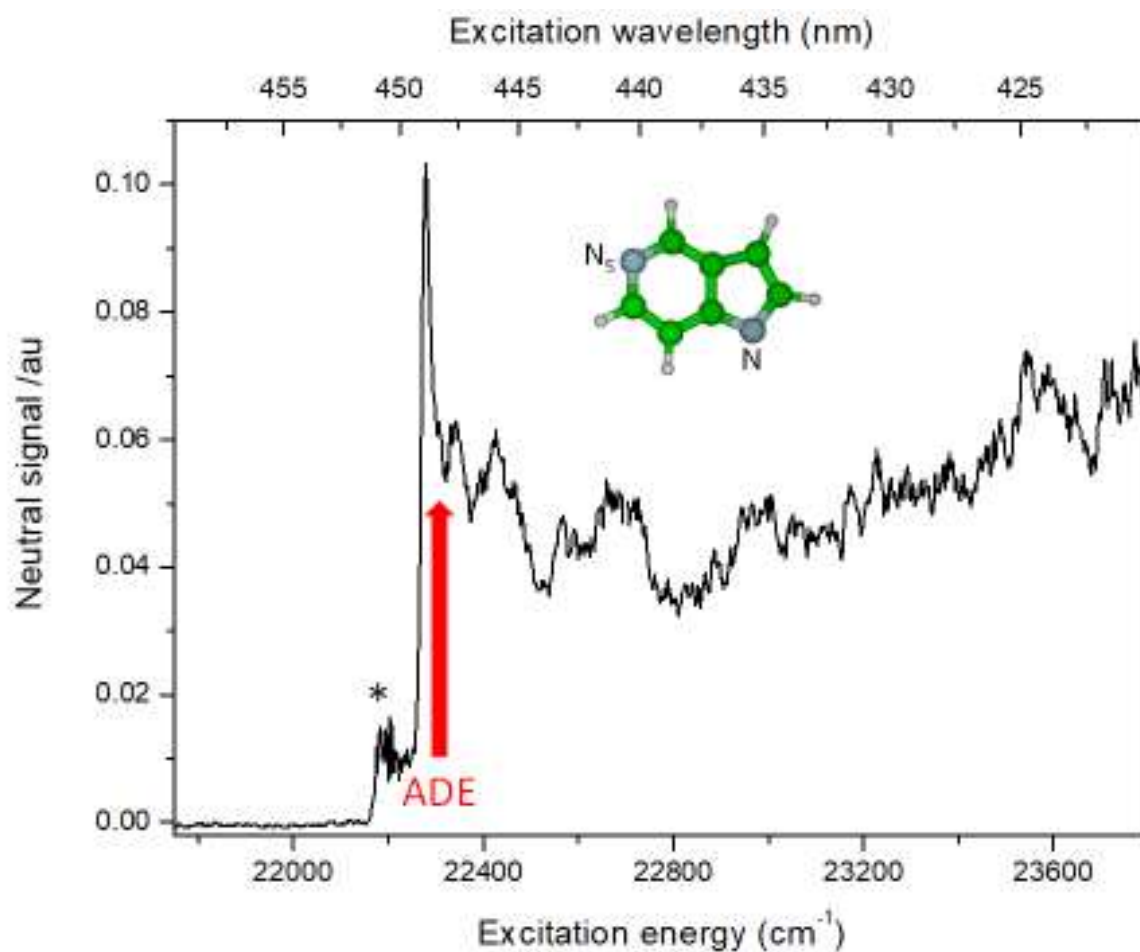


Figure 2: PD spectrum of the 5-azaindole anion recorded by following the yield of the $[5\text{-AI-H}]^*$ neutral. The ESI source was quite unstable, leading to fluctuation of the continuum signal despite strong averaging

The photodetachment spectrum of the 5-azaindole anion is presented in Figure 2. The threshold is found at $\text{ADE} = 2.82 \text{ eV}$ (22778 cm^{-1}), i.e. 0.38 eV higher in energy than that obtained for indolide. As in the case of indolide anions, the threshold of $[5\text{-AI-H}]^-$ presents a marked peak-like shape, which is only observed at the threshold and not at higher energy. No evidence of DBSs could be observed in

the spectrum, and similarly to the indole case, a small step at -100 cm^{-1} from the main threshold is observed and attributed to vibrational excitation during extraction from the trap.

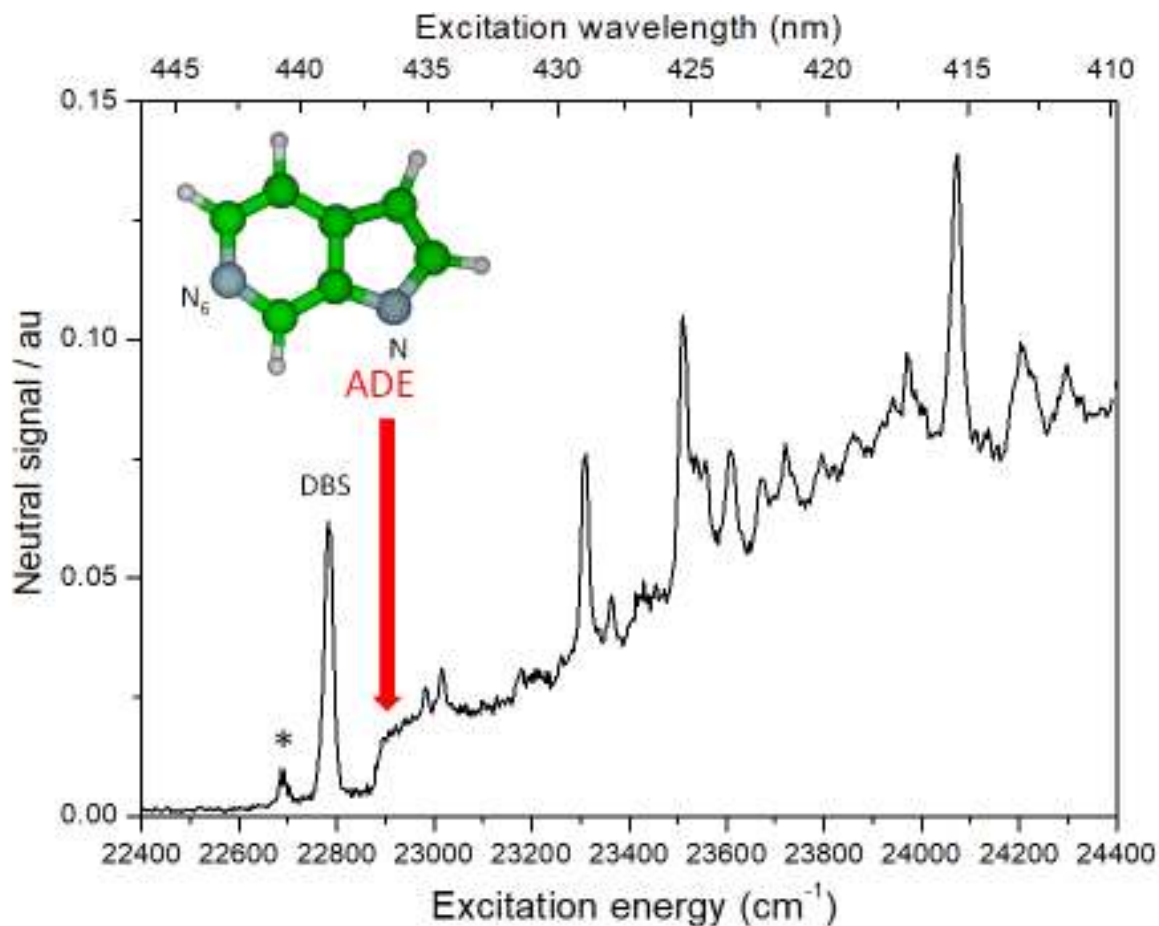


Figure 3: PD spectrum of 6-azaindole anion by following the yield of the $[6\text{-AI-H}]^*$ neutral. The arrow indicates the PD threshold; DBS designates an excitation to a dipole-bound state. The band marked with * is probably a hot band.

The photodetachment spectrum of the 6-azaindole anion is presented in Figure 3. A step-like threshold is observed at 22880 cm^{-1} (2.38 eV , 520.94 nm) and the shape of the signal corresponds to what one would expect for a “normal threshold”, according to the Wigner Threshold Law, i.e. a step. At lower energy, a DBS starting at 22780 cm^{-1} , i.e. 100 cm^{-1} below the photodetachment threshold, is observed. This band has been assigned to the DBS 0-0 band, which should not be seen in the absence of collisions (as discussed later). A smaller band starting at 22680 cm^{-1} , i.e. 100 cm^{-1} below the main band, is also observed. In addition to the photodetachment continuum, vibrational bands are evident in the spectrum, and they can be assigned to auto-detached vibrational bands of the dipole-bound anion (vide infra). The intensity of the DBS 0-0 band cannot be compared to the intensity of the other vibrations because the electron detachment mechanism is different in each case.

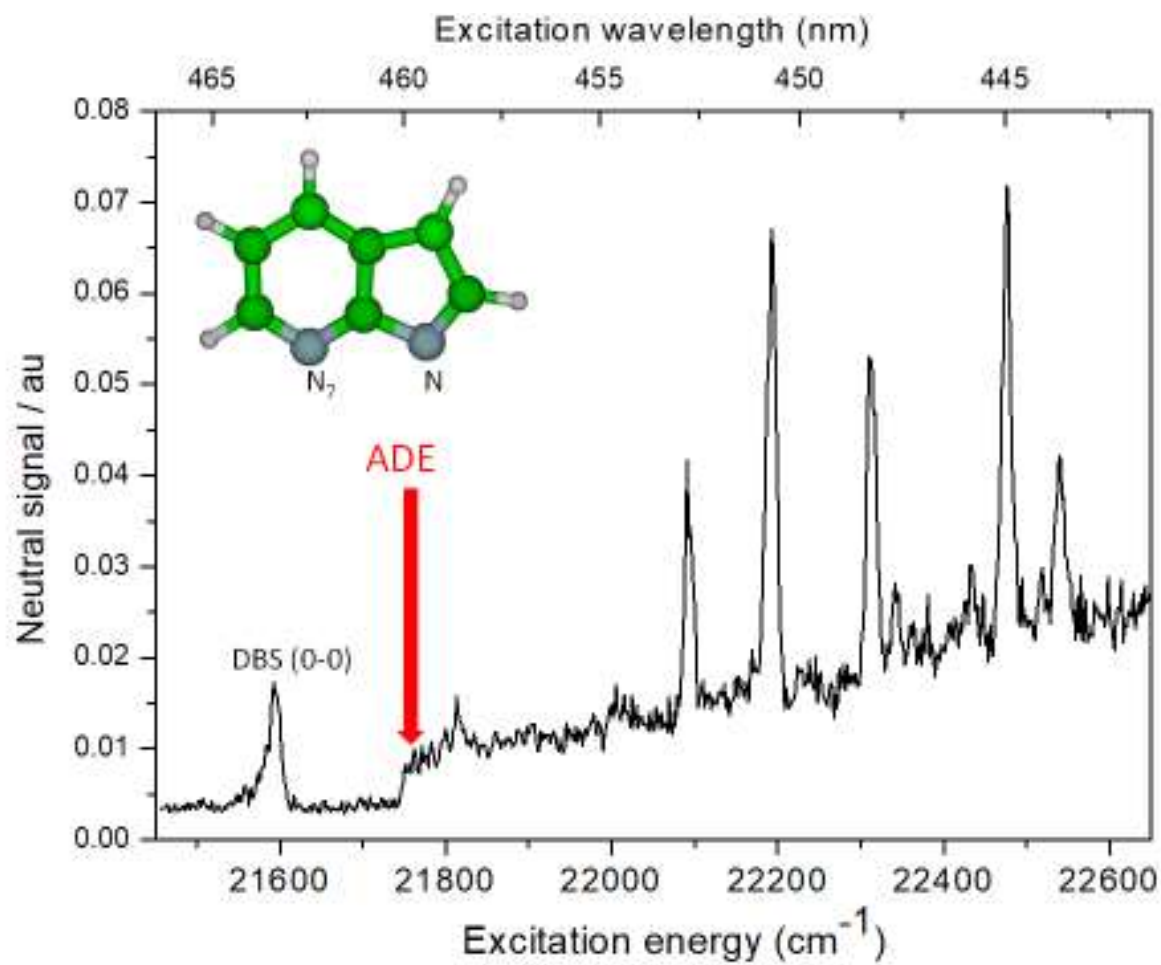


Figure 4: PD spectrum of 7-azaindole anion recorded by following the yield of the $[7\text{-AI-H}]^*$ neutral. The arrow indicates the PD threshold; DBS designates an excitation to a dipole-bound state.

The low-energy part of the 7-azaindole PD spectrum is shown in

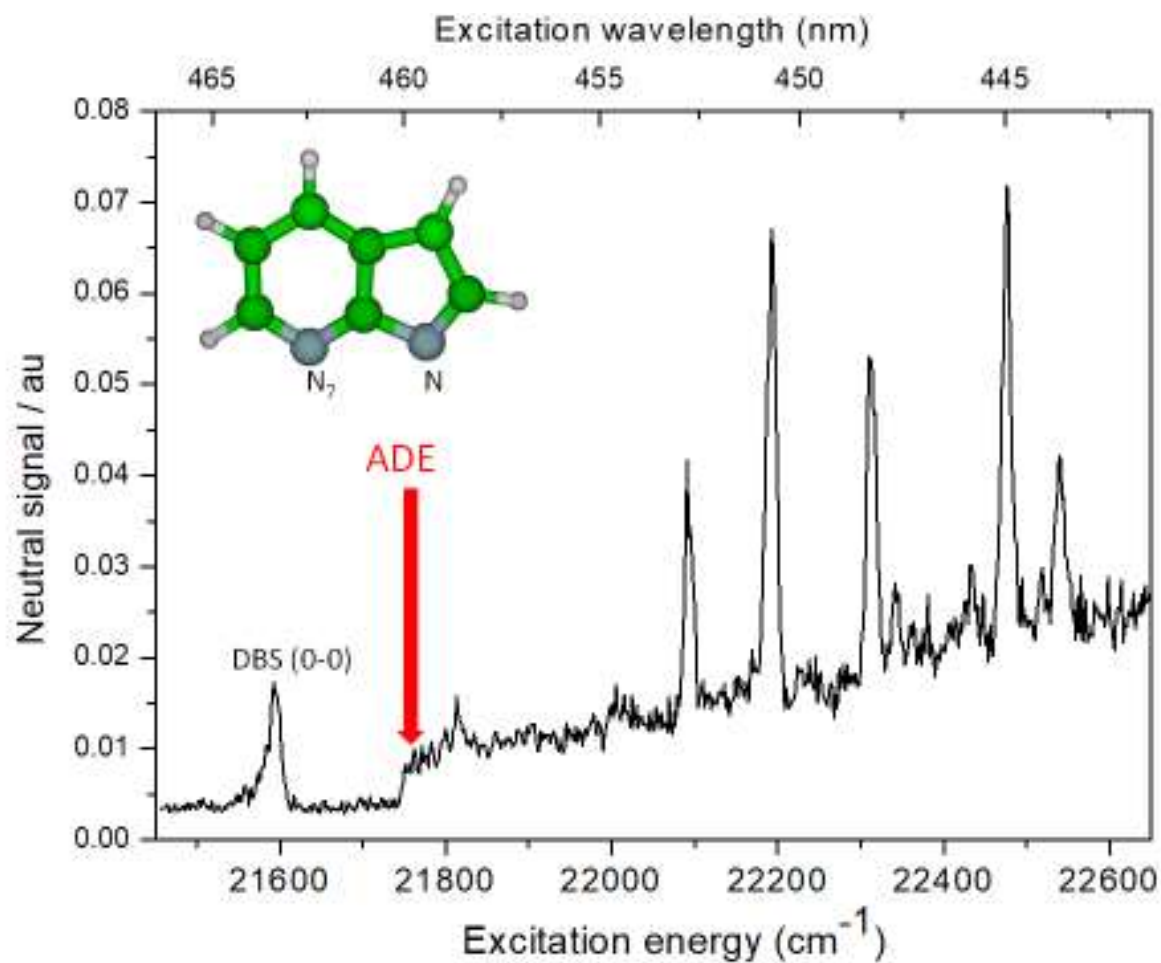


Figure 4. A photodetachment onset is observed at 21750 cm^{-1} (2.70 eV , 459.20 nm) and, as for of the 6-azaindole anion, several vibrational bands ascribed to a DBS are identified, starting at 21595 cm^{-1} (DBS 0-0 band), i.e. $-160\pm 10\text{ cm}^{-1}$ below the photodetachment threshold.

-Calculated structures and energies of anions and radicals

The structure of all the deprotonated anions studied in this work corresponds to the loss of the most acidic proton of the indolic skeleton, namely that bonded to N_1 in the five-membered ring. The resulting anions have an even number of electrons and quite similar electronic configuration ($\dots \pi(4a'')^2, \pi(5a'')^2$) independent of the N substitution. These two highest π molecular orbitals are delocalised throughout the molecule. In order to reproduce the photodetachment process, one electron has to be removed from the HOMO, producing the X^2A'' ground state of the radical. The electronic transition toward the radical is then well represented as: $X^2A'' \leftarrow X^1A'$. The experimental and calculated electronic properties are summarised in Table 1. For all the molecules studied, both the anion and the radical are planar.

Photodissociation process	ADE (eV) experimental	ADE (eV) calculated	Dipole moment of the radical (D)
indolide → indolyl + e ⁻	2.417	2.34	2.50
7-azaindolide → 7-azaindolyl + e ⁻	2.697	2.62	4.64
6-azaindolide → 6-azaindolyl + e ⁻	2.830	2.77	3.81
5-azaindolide → 5-azaindolyl + e ⁻	2.76	2.68	1.82

Table 1. Experimental and calculated ADE values, and dipole moments of the radicals calculated at the CAM-B3LYP/aug-cc-pVDZ level.

The excited state manifolds of the studied anions are quite rich (typically 15 states within 3-5 eV) as compared to what is observed in either neutral or protonated aromatic molecules of the same kind, which have only three electronic states or fewer in an equivalent spectral range. In Table 2, we give only the first three states, calculated at the CAM-B3LYP/aug-cc-pVDZ level, for all the anions of interest. As an illustration, in Figure SI-1 we compare the calculated excited states of the deprotonated indole anion (22 states up to 225 nm) against the experimental spectrum, where the main observed band at 235 nm can be assigned to the calculated S₁₉ [π (HOMO) – π^* LUMO+12] transition, with an energy of 5.32 eV (232 nm) and a very strong oscillator strength of 0.24.

Excited state	Deprotonated anion			
	7-azaindolide	6-azaindolide	5-azaindolide	Indolide
S1	2.98	3.17	3.47	2.89
S2	3.21	3.45	3.73	3.04
S3	3.49	3.74	4.11	3.24

Table 2. Calculated values of the first three excited states of the anions calculated at the CAM-B3LYP/aug-cc-pVDZ level (in eV).

The excited states in the anion are calculated well above the ADE threshold, and hence they cannot account for the observed band near the ADE threshold in the 6- and 7-azaindolide anions. None of these states could be clearly identified in the spectra due to their weak oscillator strengths. In these systems, only shape resonances²³ can be expected, which will be very broad and not easy to evidence.

Discussion

-Adiabatic Detachment Energy (ADE)

Returning to Table 1, it is interesting to discuss why the ADE values of *n*-azaindolide anions were found to be larger than that of the unsubstituted indolide by roughly 0.3 eV, the largest being the ADE of 6-azaindolide. The calculated values, which are in good agreement with the experimental values (being, on average, lower by 0.07 eV, and ruling out the possibility that this variation is attributable to the much lower Δ ZPE), also show the same tendency. A rudimentary explanation as to why azaindolide

anions have larger ADE values than indolide might be obtained by looking at the electrostatic potential map of the corresponding neutral radicals, as presented in Figure 5.

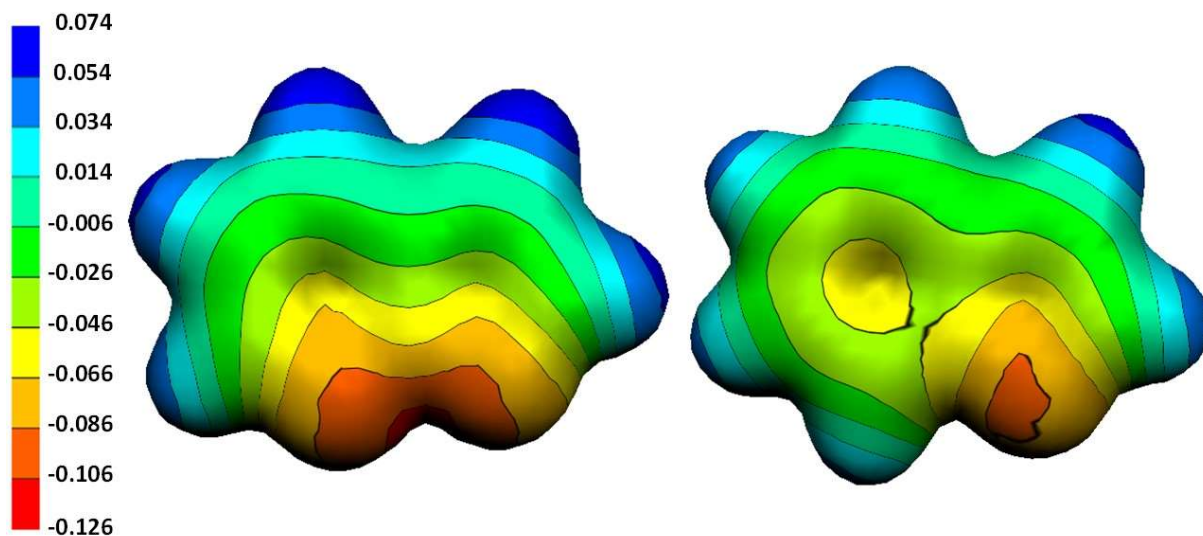


Figure 5: Electrostatic potential map for the 7-azaindoyl (left) and indoyl (right) radicals. Blue denotes an electron-deficient region while red denotes an electron-rich region. The plot was made with molekel.⁵²

By analysing the colour map (Figure 5) it is possible to recognise the strong electron attraction of the two nitrogen atoms in 7-azaindoyl (red, negative charge density of around $-0.3 e$). It can be observed that the electron charge is largely withdrawn from the hydrogen-atoms on the carbon atoms (blue), evidencing a stronger positive charge density region in 7-azaindoyl than in indoyl. It is precisely this positive charge excess on the carbon hydrogen-atoms what accounts for the increase in the binding energy of the extra electron required to form the anion.

-Dipole-bound States.

It is generally expected that any molecule with a dipole moment larger than 2.5 D can lead to the formation of a stable dipole-bound anion^{13,14,16,17,18,19,20}. In our experiments, excitations to DBSs are clearly observed for the $[7\text{-AI-H}]^-$ and $[6\text{-AI-H}]^-$ anions. The binding energies measured for these bound states are 160 cm^{-1} for the 7-isomer and 100 cm^{-1} for the 6-isomer, which is consistent with the larger dipole moment of $[7\text{-AI-H}]^*$ compared to $[6\text{-AI-H}]^*$ (see Table 1). These values are also in line with those tabulated by Desfrancois et al.¹⁶ or with what has been observed for the phenoxy radical, which has a dipole moment of 4 D and a DBS binding energy of 97 cm^{-1} .¹⁸ An important point to note is that the 0-0 band of the DBS should not be visible upon a one photon excitation process, although it could be observed if two photons are involved in the excitation. The second possibility is that the observed DBS band is induced by collisions, owing to the large size of the electron cloud which implies a large collisional cross section. It should be mentioned that the intensity of this 0-0 DBS band cannot be compared to the higher vibrational bands because, as will be discussed later, they are produced by auto-ionisation.

-Photodetachment threshold for indolide and 5-azaindolide.

The shape of the ADE thresholds of both indolide and 5-azaindolide anions is quite special because the Wigner law⁵¹ is not followed and, instead, a kind of resonance band is clearly observed at the threshold. Such a resonance is not seen when the DBS is well stabilised (as in 7- and 6-azaindolide, or uracil¹⁹). Moreover, no vibrational bands associated with this resonance are detected at higher energy, contrary to what is observed for 6-azaindolide and 7-azaindolide, where spectral bands above the threshold were assigned to vibrational states of the dipole-bound species.

A possible explanation for these observations would be the presence of a very weakly dipole-bound state (with an energy of a few cm^{-1}) that we cannot spectrally resolve with our laser resolution of 10 cm^{-1} . It would be interesting to repeat the experiment with a higher spectral resolution to test this possibility.

For 5-azaindolide, a weak threshold is observed at -100 cm^{-1} below the main threshold. We will discuss the origin of this spectral feature in terms of several plausible processes. The first possibility is to assign it to a hot band, although it cannot be a $v''=0$ vibration because there is no such low frequency in the anion (the lowest being at 225 cm^{-1}). It could also be a sequence of vibrations $X''=1$ to $X'=1$, but in that case the vibration should change by 100 cm^{-1} between the anion and the radical, and we did not calculate such a frequency change. The radical being a doublet state, some spin orbit states can exist, but as the spin orbit constant of the N-atom is in the order of 15 cm^{-1} ,⁵³⁵⁴ this does not seem to be the right order of magnitude. The absorption might also be an excited state of the anion, with the neutral produced being the fragment of the dissociating anion, but no charged fragment was detected upon excitation in the ion trap, and the excited states are not calculated to lie in this energy region (the lowest excited state being calculated at 3.4 eV , i.e. 0.6 eV higher in energy than the ADE). In light of the above discussion, we do not currently have a definitive explanation for this band.

-DBS vibrational spectra

We mentioned that the bands observed in the 6- and 7-azaindolyl spectra can be assigned to vibrations of the DBSs that arise from the excitation of the 6- and 7-azaindolide anions. Since we are only detecting neutral molecules, these vibrations must originate in vibrational auto-ionisation of vibrationally-excited bound states. The width of this type of band is around 10 cm^{-1} , and hence the measurement is limited by the spectral width of our laser, which unfortunately precludes the study of the rotational structure and measurement of the auto-ionisation rate, as done for similar experiments on deprotonated uracil¹⁹ or phenoxyde¹⁸ anions.

The assignment of the vibrational spectra is deduced from the ab-initio calculations and the values are given in Tables SI-1 and SI-2. Simulated spectra, obtained using the pGopher program, are presented in Figure 6 alongside the experimental spectra. From this simulation it appears that the 0-0 band is by far the most intense band, showing that the change of geometry between the radical and the deprotonated anion is not that large. This is not observed in the experimental spectra since the 0-0 band is not produced by the same process (auto-ionisation) as the higher vibrational states. As expected, the observed vibrations are mostly of A' symmetry, except for bands around 200 cm^{-1} , with such small frequencies corresponding to out of plane vibrations. These bands with A'' symmetry should

not be seen in the FC approximation, and they are probably visible due to vibrational coupling with an excited state.

The comparison between the experimental data and the calculations is not as good as what one can achieve for closed-shell structure species (see, for example, the protonated azaindole molecules [ref Noble+2020 AIH+], but they are reasonable, as one can see in comparing the calculated values with the experimental ones. The main discrepancy arises in the lowest in-plane vibration at around 500 cm^{-1} , which has too weak an intensity in the simulation.

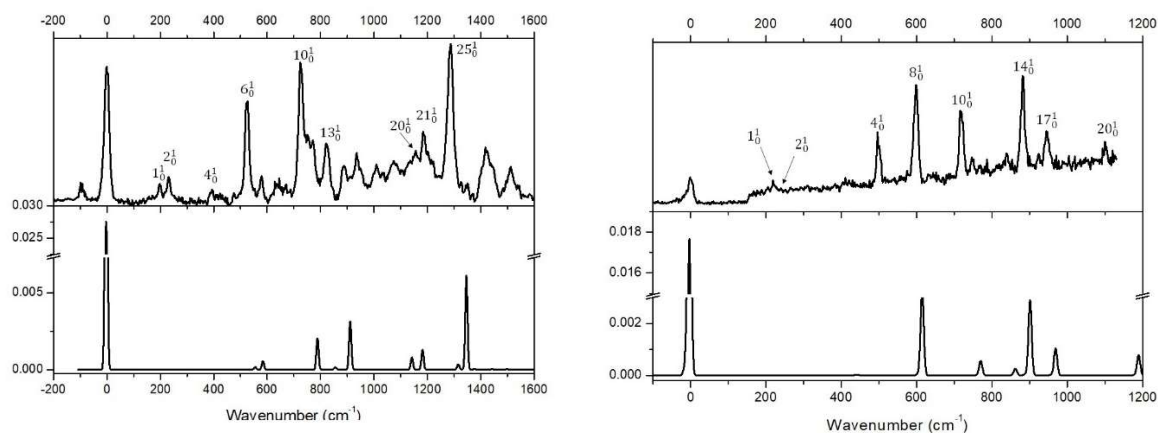


Figure 6 Experimental and simulated spectra of 6-azaindoyl (left) and 7-azaindoyl (right) radicals. The observed frequencies are tabulated in Table 3.

6-azaindoyl [6-AI-H] [•] vibrations		
number	experimental	calculated
1 a ^{''}	197	208
2 a ^{''}	230	240
4 a [']	397	404
6 a [']	527	559
10 a [']	724	792
13 a [']	821	859
20 a [']	1153	1146
21 a [']	1184	1181
25 a [']	1288	1350

7-azaindoyl [7-AI-H] [•] vibrations		
number	experimental	calculated
1 a ^{''}	219	218
4 a [']	499	445
8 a [']	601	618
10 a [']	717	774
14 a [']	884	866
17 a [']	947	907
20 a [']	1162	1197

Table 3: Experimental and calculated vibrational bands of the 6-azaindoyl and 7-azaindoyl radicals

-Comparison between anion and radical vibrations

In Figure 7, the difference in frequencies between the anion and the radical is presented for the two symmetries A' (in-plane) and A'' (out-of-plane). Positive values indicate that the frequency of the anion is larger than that of the radical. There are both positive and negative values calculated for

the frequency differences in both the in-plane and out-of-plane modes. Looking at the normal modes, one can observe that the frequencies which are larger in the anions are those concerning the indole ring and the frequencies which are smaller in the anions concern those localised on the CH or NH modes. One can conclude that the indole plane is more rigid in the anion (closed shell structure) than in the radical, while the CH/NH bonds are stronger in the radical than in the anion.

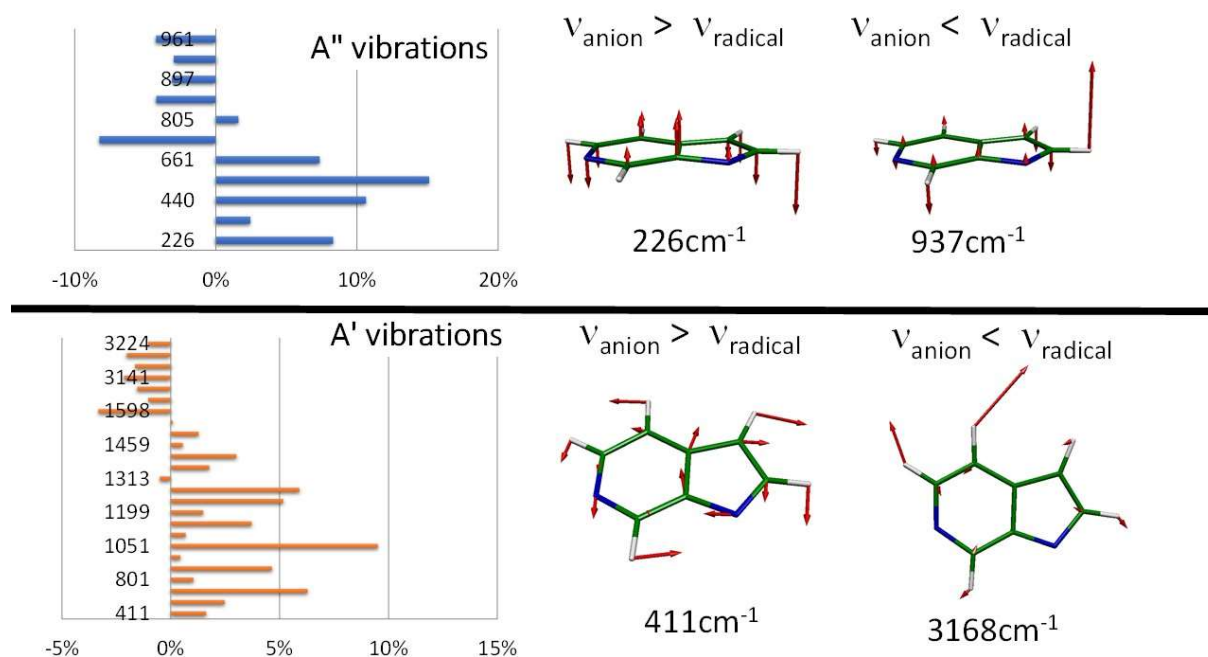


Figure 7: Comparison of vibrations between the deprotonated anion and the radical for 6-azaindole. Left: frequency difference between the anion and the radical (in per cent) for the A'' and A' modes. The modes which include the motion of the heavy atoms of the ring are smaller in the radical. Conversely, the modes in which the H atom motion is preponderant are larger. Right: typical vibrations of A'' and A' modes are presented; at low frequencies, vibrations of anion > vibrations of radical, while at high frequency vibrations of anion < vibrations of radical

A comparison between the vibrations of the deprotonated, protonated and neutral molecular forms is not straightforward because they don't have the same number of atoms. However, in the calculations performed for each species the CH vibrations can be clearly identified, and it appears that these vibrations have the highest frequencies for the protonated species (on average $3250 \pm 20 \text{ cm}^{-1}$) [ref Noble+2020 AIH+], and the lowest for the deprotonated anions ($2.5 \pm 0.5 \%$ lower), with intermediate values for the neutrals (1.5% lower) and the deprotonated radicals (0.8% lower).

Conclusions

We have investigated the cold deprotonated anions of indole and 5-, 6-, and 7-azaindole. Upon photoexcitation, we did not observe a clear signature of the excited states of the anion, which are all calculated to lie above the adiabatic detachment energy, nor did we observe photofragmentation of the anions. The photodetachment thresholds were detected, and the analysis of the time of flight profile of the neutral radicals produced after photodetachment indicates that the radicals do not fragment, i.e. similar behaviour to that observed for the tryptophan anion when it is deprotonated on the indolic cycle. For the 6- and 7-azaindole anions (dipole > 3.8 D), dipole-bound states were observed,

whereas for the indole and 5-azaindole anions (dipole < 2.5 D), the shape of the ionisation threshold seems to indicate the presence of a very weakly bound DBS that cannot be resolved at the spectral resolution of our laser.

Acknowledgments

This work has been conducted within the International Associated Laboratory LEMIR (CNRS/CONICET) and was supported by CONICET, FONCyT, SeCyT-UNC, CNRS (INSIS), and the ANR Research Grant (ANR2010BLANC040501-ESPEM and ANR17CE05000502-Wsplit). We also acknowledge the use of the computing facility cluster Meso-LUM of the LUMAT federation (LUMAT FR 2764).

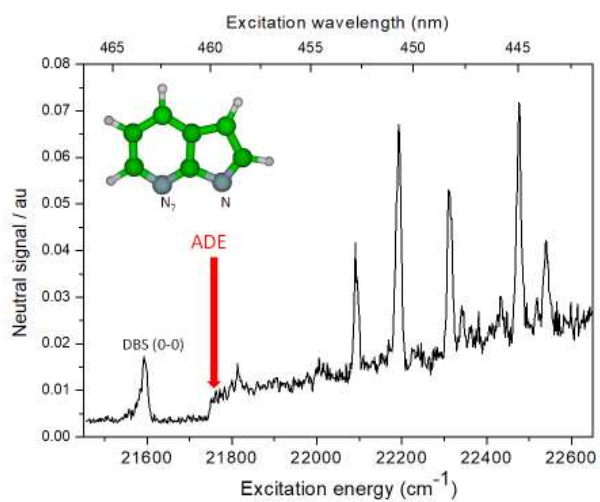
Bibliography

- 1 J. T. Vivian and P. R. Callis, Mechanisms of tryptophan fluorescence shifts in proteins., *Biophys. J.*, 2001, **80**, 2093–109.
- 2 D. M. Chudakov, M. V. Matz, S. Lukyanov and K. A. Lukyanov, Fluorescent proteins and their applications in imaging living cells and tissues, *Physiol. Rev.*, 2010, **90**, 1103–1163.
- 3 K. S. Sarkisyan, I. V. Yampolsky, K. M. Solntsev, S. A. Lukyanov, K. A. Lukyanov and A. S. Mishin, Tryptophan-based chromophore in fluorescent proteins can be anionic, *Sci. Rep.*, 2012, **2**, 1–5.
- 4 L. Merkel, M. G. Hoesl, M. Albrecht, A. Schmidt and N. Budisa, Blue fluorescent amino acids as in vivo building blocks for proteins, *ChemBioChem*, 2010, **11**, 305–314.
- 5 D. J. Nelson, A. M. Oliveira and W. C. Lineberger, Anion photoelectron spectroscopy of deprotonated indole and indoline, *J. Chem. Phys.*, 2018, **148**, 1–8.
- 6 G. A. Pino, R. A. Jara-Toro, J. P. Aranguren-Abrate, C. Dedonder-Lardeux and C. Jouvét, Dissociative photodetachment vs. photodissociation of aromatic carboxylates: the benzoate and naphthoate anions, *Phys. Chem. Chem. Phys.*, 2019, **21**, 1797–1804.
- 7 L.-S. Wang, Perspective: Electrospray photoelectron spectroscopy: From multiply-charged anions to ultracold anions, *J. Chem. Phys.*, 2015, **143**, 040901.
- 8 J. N. Bull, J. T. Buntine, M. S. Scholz, E. Carrascosa, L. Giacomozzi, M. H. Stockett and E. J. Bieske, Photodetachment and photoreactions of substituted naphthalene anions in a tandem ion mobility spectrometer, *Faraday Discuss.*, 2019, **217**, 34–46.
- 9 G. A. Pino, I. Alata, C. Dedonder, C. Jouvét, K. Sakota and H. Sekiya, Photon induced isomerization in the first excited state of the 7-azaindole-(H₂O)₃ cluster., *Phys. Chem. Chem. Phys.*, 2011, **13**, 6325–6331.
- 10 K. Sakota, C. Jouvét, C. Dedonder, M. Fujii and H. Sekiya, Excited-state triple-proton transfer in 7-azaindole(H₂O)₂ and reaction path studied by electronic spectroscopy in the gas phase and quantum chemical calculations, *J. Phys. Chem. A*, 2010, **114**, 11161–11166.
- 11 N. Kungwan, K. Kerdpol, R. Daengngern, S. Hannongbua and M. Barbatti, Effects of the second hydration shell on excited-state multiple proton transfer: Dynamics simulations of 7-azaindole: (h₂o)₁₋₅ clusters in the gas phase, *Theor. Chem. Acc.*, 2014, **133**, 1–11.
- 12 Y. Koizumi, C. Jouvét, T. Norihiro, S. Ishiuchi, C. Dedonder-Lardeux and M. Fujii, Electronic spectra of 7-azaindole/ammonia clusters and their photochemical reactivity, *J. Chem. Phys.*, 2008, **129**, 101411.
- 13 J. Marks, J. I. Brauman, R. D. Mead, K. R. Lykke and W. C. Lineberger, Spectroscopy and dynamics of the dipole-supported state of acetyl fluoride enolate anion, *J. Chem. Phys.*, 1988, **88**, 6785–6792.
- 14 R. D. Mead, K. R. Lykke, W. C. Lineberger, J. Marks and J. I. Brauman, Spectroscopy and dynamics of the dipole-bound state of acetaldehyde enolate, *J. Chem. Phys.*, 1984, **81**, 4883–4892.
- 15 J. A. Noble, J. P. Aranguren-abate, C. Dedonder, C. Jouvét and G. A. Pino, Photodetachment of deprotonated aromatic amino acids : stability of the dehydrogenated radical depends on the deprotonation site, *Phys. Chem. Chem. Phys.*, 2019, **21**, 23346–23354.
- 16 C. Desfrancois, H. Abdoul-Carime, N. Khelifa and J. P. Schermann, From 1r to 1r₂ potentials: Electron exchange between Rydberg atoms and polar molecules, *Phys. Rev. Lett.*, 1994, **73**, 2436–2439.
- 17 C. Desfrancois, H. Abdoul-Carime and J.-P. Schermann, Ground state dipole bound anions, *Int. J. Mod. Physic B*, 1996, **10**, 1339–1395.
- 18 H.-T. Liu, C.-G. Ning, D.-L. Huang, P. D. Dau and L.-S. Wang, Observation of Mode-Specific Vibrational Autodetachment from Dipole-Bound States of Cold Anions, *Angew. Chemie*, 2013, **125**, 9146–9149.
- 19 H.-T. T. Liu, C.-G. G. Ning, D.-L. L. Huang and L.-S. S. Wang, Vibrational spectroscopy of the dehydrogenated uracil radical by autodetachment of dipole-bound excited states of cold anions, *Angew. Chemie - Int. Ed.*, 2014, **53**, 2464–2468.
- 20 D. L. Huang, H. T. Liu, C. G. Ning and L. S. Wang, Conformation-selective resonant photoelectron

- spectroscopy via dipole-bound states of cold anions, *J. Phys. Chem. Lett.*, 2015, **6**, 2153–2157.
- 21 G. Z. Zhu, C. H. Qian and L. S. Wang, Dipole-bound excited states and resonant photoelectron imaging of phenoxide and thiophenoxide anions, *J. Chem. Phys.*, DOI:10.1063/1.5049715.
- 22 R. E. Continetti and H. Guo, Dynamics of transient species via anion photodetachment, *Chem. Soc. Rev.*, 2017, **46**, 7650–7667.
- 23 J. Schiedt and R. Weinkauff, Resonant photodetachment via shape and Feshbach resonances: P-benzoquinone anions as a model system, *J. Chem. Phys.*, 1999, **110**, 304–314.
- 24 S. J. Kregel and E. Garand, Ground and low-lying excited states of phenoxy, 1-naphthoxy, and 2-naphthoxy radicals via anion photoelectron spectroscopy, *J. Chem. Phys.*, 2018, **149**, 0–9.
- 25 H. Li, Z. Lin and Y. Luo, Gas-phase IR spectroscopy of deprotonated amino acids: Global or Local minima?, *Chem. Phys. Lett.*, 2014, **598**, 86–90.
- 26 X. Bin Wang, C. F. Ding and L. S. Wang, Photodetachment spectroscopy of a doubly charged anion: Direct observation of the repulsive coulomb barrier, *Phys. Rev. Lett.*, 1998, **81**, 3351–3354.
- 27 Z. Tian, X.-B. Wang, L.-S. Wang and S. R. Kass, Are Carboxyl Groups the Most Acidic Sites in Amino Acids? Gas-Phase Acidities, Photoelectron Spectra, and Computations on Tyrosine, p-Hydroxybenzoic Acid, and Their Conjugate Bases, *J. Am. Chem. Soc.*, 2008, **131**, 1174–1181.
- 28 I. Alata, J. Bert, M. Broquier, C. Dedonder, G. Féraud, G. Grégoire, S. Soorkia, E. Marceca and C. Juvet, Electronic spectra of the protonated indole chromophore in the gas phase., *J. Phys. Chem. A*, 2013, **117**, 4420–7.
- 29 H. Kang, G. Féraud, C. Dedonder-lardeux and C. Juvet, New Method for Double-Resonance Spectroscopy in a Cold Quadrupole Ion Trap and Its Application to UV – UV Hole-Burning Spectroscopy of Protonated Adenine Dimer, *J. Phys. Chem. Lett.*, 2014, **5**, 2760.
- 30 G. Féraud, C. Dedonder, C. Juvet, Y. Inokuchi, T. Haino, R. Sekiya and T. Ebata, Development of Ultraviolet – Ultraviolet Hole-Burning Spectroscopy for Cold Gas-Phase Ions, *J. Phys. Chem. Lett.*, 2014, **5**, 1236–1240.
- 31 M. Barat, J. C. Brenot, J. A. Fayeton and Y. J. Picard, Absolute detection efficiency of a microchannel plate detector for neutral atoms, *Rev. Sci. Instrum.*, 2000, **71**, 2050.
- 32 J. A. Noble, J. P. Aranguren-Abate, C. Dedonder, C. Juvet and G. A. Pino, Photodetachment of deprotonated aromatic amino acids: Stability of the dehydrogenated radical depends on the deprotonation site, *Phys. Chem. Chem. Phys.*, 2019, **21**, 23346–23354.
- 33 L. Lammich, M. A. Petersen, M. B. Nielsen and L. H. Andersen, The gas-phase absorption spectrum of a neutral GFP model chromophore., *Biophys. J.*, 2007, **92**, 201–7.
- 34 R. Cercola, E. Matthews and C. E. H. Dessent, Photoexcitation of Adenosine 5'-Triphosphate Anions in Vacuo: Probing the Influence of Charge State on the UV Photophysics of Adenine, *J. Phys. Chem. B*, 2017, **121**, 5553–5561.
- 35 C. S. Anstöter and J. R. R. Verlet, Gas-Phase Synthesis and Characterization of the Methyl-2,2-dicyanoacetate Anion Using Photoelectron Imaging and Dipole-Bound State Autodetachment, *J. Phys. Chem. Lett.*, 2020, **11**, 6456–6462.
- 36 M. W. Forbes and R. A. Jockusch, Deactivation pathways of an isolated green fluorescent protein model chromophore studied by electronic action spectroscopy, *J. Am. Chem. Soc.*, 2009, **131**, 17038–17039.
- 37 S. B. Nielsen, A. Lapiere, J. U. Andersen, U. V. Pedersen, S. Tomita and L. H. Andersen, Absorption spectrum of the green fluorescent protein chromophore anion in vacuo, *Phys. Rev. Lett.*
- 38 T. R. Rizzo, J. A. Stearns and O. V. Boyarkin, Spectroscopic studies of cold, gas-phase biomolecular ions, *Int. Rev. Phys. Chem.*, 2009, **28**, 481.
- 39 M. Z. Kamrath, R. a. Relph, T. L. Guasco, C. M. Leavitt and M. a. Johnson, Vibrational predissociation spectroscopy of the H₂-tagged mono- and dicarboxylate anions of dodecanedioic acid, *Int. J. Mass Spectrom.*, 2010, **300**, 91–98.
- 40 Y. Inokuchi, T. Haino, R. Sekiya, F. Morishima, C. Dedonder, G. Raldine, F. Raud, C. Juvet and T. Ebata, UV photodissociation spectroscopy of cryogenically cooled gas phase host guest complex

- ions of crown ethers, *Phys. Chem. Chem. Phys.*, 2015, **17**, 25925–25934.
- 41 H. Wako, S. Ishiuchi, D. Kato, G. Feraud, C. Dedonder-Lardeux, C. Jouvet and M. Fujii, Conformational study of protonated noradrenaline by UV-UV and IR dip double resonance laser spectroscopy combined with an electrospray and a cold ion trap methods, *Phys. Chem. Chem. Phys.*, 2017, **19**, 10777–10785.
- 42 E. N. Sullivan, B. Nichols and D. M. Neumark, Fast beam photofragment translational spectroscopy of the phenoxy radical at 225 nm, 290 nm, and 533 nm, *Phys. Chem. Chem. Phys.*, 2019, **21**, 14270–14277.
- 43 J. Houmøller, M. Wanko, K. Støchkel, A. Rubio and S. Brøndsted Nielsen, On the effect of a single solvent molecule on the charge-transfer band of a donor-acceptor anion, *J. Am. Chem. Soc.*, 2013, **135**, 6818–6821.
- 44 V. Lepere, B. Lucas, M. Barat, J. A. Fayeton, Y. J. Picard, C. Jouvet, P. Çarçal, I. B. Nielsen, C. Dedonder-Lardeux, G. Grégoire and A. Fujii, Characterization of neutral fragments issued from the photodissociation of protonated tryptophane., *Phys. Chem. Chem. Phys.*, 2007, **9**, 5330–5334.
- 45 S. S. Kumar, M. Pérot-Taillandier, B. Lucas, S. Soorkia, M. Barat and J. a Fayeton, UV photodissociation dynamics of deprotonated 2'-deoxyadenosine 5'-monophosphate [5'-dAMP-H]-., *J. Phys. Chem. A.*, 2011, **115**, 10383–90.
- 46 E. Matthews, R. Cercola, G. Mensa-Bonsu, D. M. Neumark and C. E. H. Dessent, Photoexcitation of iodide ion-pyrimidine clusters above the electron detachment threshold: Intracluster electron transfer versus nucleobase-centred excitations, *J. Chem. Phys.*, , DOI:10.1063/1.5018168.
- 47 M. W. Forbes, A. M. Nagy and R. a. Jockusch, Photofragmentation of and electron photodetachment from a GFP model chromophore in a quadrupole ion trap, *Int. J. Mass Spectrom.*, 2011, **308**, 155–166.
- 48 M. J. Frisch, G. W. Trucks, H. B. Schlegel, G. E. Scuseria, M. A. Robb, J. R. Cheeseman, V. G. Zakrzewski, J. A. Montgomery, R. E. Stratmann, J. C. Burant, S. Dapprich, J. M. Millam, A. D. Daniels, K. N. Kudin, M. C. Strain, O. Farkas, J. Tomasi, V. Barone, M. Cossi, R. Cammi, B. Mennucci, C. Pomelli, C. Adamo, S. Clifford, J. Ochterski, G. A. . Petersson, P. Y. Ayala, Q. Cui, K. Morokuma, D. K. Malick, A. D. . Rabuck, K. Raghavachari, J. B. Foresman, J. Cioslowski, J. V Ortiz, B. B. Stefanov, G. Liu, A. Liashenko, P. Piskorz, I. Komaromi, R. Gomperts, R. L. Martin, D. J. Fox, T. Keith, M. A. Al-Laham, C. Y. Peng, A. Nanayakkara, C. Gonzalez, M. Challacombe, P. M. W. Gill, B. G. Johnson, W. Chen, M. W. Wong, J. L. Andres, M. Head-Gordon, E. S. Replogle, J. A. Pople, M. W. Schmidt, E. K. K. Baldrige, J. A. Boatz, S. T. Elbert, M. S. Gordon, J. H. Jensen, S. Koseki, N. Matsunaga, K. A. Nguyen, S. J. Su, T. L. Windus and M. DuPuis, ., *Gaussian 09; Gaussian, Inc. Pittsburgh, PA.*
- 49 *PGOPHER, a Progr. Simulating Rotational Struct. C. M. West. Univ. Bristol, <http://pgopher.chm.bris.ac.uk>.*
- 50 L. Giacomozzi, C. Kjær, J. Langeland Knudsen, L. H. Andersen, S. Brøndsted Nielsen and M. H. Stockett, Absorption and luminescence spectroscopy of mass-selected flavin adenine dinucleotide mono-anions, *J. Chem. Phys.*, , DOI:10.1063/1.5024028.
- 51 E. P. Wigner, On the Behavior of Cross Sections Near Thresholds, *Phys. Rev.*, 1948, 1002–1009.
- 52 U. Varetto, MOLEKEL 4.3; Swiss National Supercomputing Centre: Manno (Switzerland), *MOLEKEL 4.3; Swiss Natl. Supercomput. Cent. Manno.*
- 53 M. Hochlaf, H. Ndome, D. Hammoutène and M. Vervloet, Valence-Rydberg electronic states of N₂: Spectroscopy and spin-orbit couplings, *J. Phys. B At. Mol. Opt. Phys.*, , DOI:10.1088/0953-4075/43/24/245101.
- 54 R. W. Field, O. Pirali and D. W. Tokaryk, The spin-orbit and rotational constants for the N₂ C'' 5Π_{ui} (v=3) state, *J. Chem. Phys.*, 2006, **124**, 5–8.
- 55 A. R. Allouche, Gabedit—A graphical user interface for computational chemistry softwares., *J. Comput. Chem.*, 2011, **32**, 174–182.

ToC Entry



Dipole bound state and its vibrational structure observed in deprotonated 7-azaindole by recording the signal of 7-azaindoly stable neutral radical